Annals of Biomedical Engineering, Vol. 40, No. 12, December 2012 *(© 2012)* pp. 2627–2638
DOI: 10.1007/s10439-012-0612-6

BMES BIOMEDICAL ENGINEERING SOCIETY™ www.bmes.org

A Statistically Based Acute Ischemia Detection Algorithm Suitable for an Implantable Device

BRUCE HOPENFELD,[1] M. SASHA JOHN,[1,2,3] TIM A. FISCHELL,[1,4] and STEVEN R. JOHNSON[1]

[1]Angel Medical Systems, 1163 Shrewsbury Avenue, Shrewsbury, NJ 07702, USA; [2]Rotman Research Institute, Baycrest Centre for Geriatric Care, Toronto, ON, Canada; [3]Institute of Biomaterials and Biomedical Engineering, University of Toronto, Toronto, ON, Canada; and [4]Borgess Heart Institute, Michigan State University, Kalamazoo, MI, Canada

(Received 24 February 2012; accepted 19 June 2012; published online 28 June 2012)

Associate Editor Stefan Jockenhoevel oversaw the review of this article.

Abstract—This study investigates the performance of a new statistically driven acute ischemia detection algorithm that can process data from two bipolar cutaneous or subcutaneous leads. During a start-up phase, the algorithm processes electrocardiogram signals to determine a normal range of ST-segment deviation as a function of heart rate. The algorithm then generates upper and lower ST-deviation thresholds based on the dispersion of the baseline ST-deviation data. After the start-up phase, persistent ST-deviation that is beyond either the upper or lower thresholds results in detection of acute ischemia. To test the algorithm, we performed long-term (10 day) Holter monitoring in a control group of 14 subjects. We also performed Holter monitoring during balloon angioplasty, and for 2 days after surgery, in 30 subjects who underwent elective percutaneous coronary interventions ("PCI"). We determined the percentage of balloon inflations the algorithm detected without producing false positive detections within the control group 10-day daily life data. The algorithm detected 17/17 LAD occlusions, 7/8 LCX occlusions, and 8/9 RCA occlusions. Our results suggest that automatically generated, subject-specific, heart-rate dependent ST-deviation thresholds can detect PCI induced myocardial ischemia without resulting in false positive detections in a small control group.

Keywords—Implantable acute ischemia monitor, ST-segment deviation, Balloon occlusion.

ABBREVIATIONS

LU	Left Up Lead
LD	Left Down Lead

Address correspondence to Bruce Hopenfeld, Angel Medical Systems, 1163 Shrewsbury Avenue, Shrewsbury, NJ 07702, USA. Electronic mail: brhopenfeld@yahoo.com

INTRODUCTION

A chronically implanted monitor that provides an early warning of acute ischemic events could greatly reduce symptom-to-treatment delays that are associated with increased risk of death and increased irreversible cardiac tissue damage. Rapid detection and treatment allows therapy to be delivered while the patient can still obtain significant benefit. This "early" intervention will predictably lead to improved patient outcomes.[4] The first implanted ischemia detection and alerting device (the "AngelMed Guardian®") is currently undergoing a pivotal FDA trial in the United States.[3,5]

This device detects ischemia by analyzing electrocardiographic (ECG) signals. Electrocardiography is acknowledged to be imperfect, but nonetheless "lies at the center of the decision pathway for the evaluation and management of patients with acute ischemic discomfort."[1,2] Specifically, clinicians analyze ST-segment shifts to diagnose acute ischemic events. Similarly, the AngelMed Guardian® detects acute ischemia by detecting abrupt changes in ST-segment voltage.[3,5] The ST-segment is the portion of an ECG signal just after the QRS complex and before the T-wave.

If a patient's ST-segment voltage is significantly elevated (>1 mm) above the iso-electric line on a 12-lead surface ECG, in two or more contiguous surface leads, the patient may be diagnosed with an ST-elevation acute myocardial infarction, also known as a "STEMI."[1,2] In contrast, if the ST-segment voltage is significantly depressed (>1 mm) below the iso-electric line on a 12-lead ECG in two or more contiguous surface leads, the patient may be diagnosed as having unstable angina (UA) or non-ST-elevation acute myocardial infarction, known as "NSTEMI." In some cases this ST-segment depression may also represent a true STEMI arising from transmural ischemia in the posterior wall of the left ventricle ("true posterior MI").

The AngelMed Guardian® was designed to detect all abrupt changes in ST-deviation regardless of the polarity of those changes, in order to alert patients of an acute ischemic event so that they may obtain further diagnosis and treatment at a hospital. This device detects acute ischemic events by applying patient-specific, statistically derived thresholds to ST-segment data, using a patient's own baseline ST-segment history as the "control." ST-segment data is derived from an electrogram recorded from a lead implanted at or near the apex of the right ventricle. A device that could utilize subcutaneous leads may obviate the potential risks that are associated with an intracardiac lead, such as intracardiac infection, cardiac tamponade, and lead fracture. However, subcutaneous signals are generally noisier than intracardiac signals, such that the algorithm employed by the AngelMed Guardian® may not be optimal for the relatively noisy subcutaneous environment.

Very few subcutaneous acute ischemia detection devices are described in the literature. Song *et al.*[10] disclose a monitor that measures ST-segment changes in two relatively short cutaneous/subcutaneous bipolar leads and that detects ischemia based on absolute voltage shifts. Stadler *et al.*[11] describe an ischemia monitor that measures ST-segment deviation by subtracting a baseline filtered ST time series from a short term filtered ST time series. Ischemia is detected based on absolute voltage criteria.

A statistical approach to ischemia detection has been implemented by Smrdel and Jager,[9] who describe a sophisticated algorithm that classifies a long term record based on a statistical analysis of the entire record. However, this algorithm is not directed to real-time acute ischemia detection, and it is more complex than is desirable for an implantable device. Similarly, the computational cost of principal component analysis based techniques[7,8] excluded them from consideration for an implantable device.

We developed a new algorithm, suitable for real time detection in an implantable device, that employs a novel statistical scheme to analyze heart-rate dependent ST-segment voltage data and that is tailored to handle the noisy subcutaneous environment. The present work first describes our algorithm, and then assesses its performance with respect to clinical Holter data collected from two non-standard bipolar body surface leads.

MATERIALS AND METHODS

Subjects

Holter data were recorded from both a healthy population of 14 volunteers ("Control group") and 30 volunteers (14 from the University of Utah in Salt Lake City, UT and 16 from Borgess Medical Center in Kalamazoo, MI) who underwent balloon inflations during percutaneous coronary interventions ("PCI group"). All of the volunteers were scheduled to undergo elective PCI. The study protocol was approved by the Institutional Review Boards of Borgess Medical Center and the University of Utah Medical Center.

Holter Recording Protocol

Control Subjects

Daily-life recordings were obtained in the Control subjects, each who were monitored nearly continuously over a 10-day period. Control subjects were allowed a break of up to 2 h per day (e.g., to take a shower) but were otherwise monitored. At least some of the Control subjects engaged in normal activities such as jogging and weight lifting, and more extreme activities such as riding on a roller coaster.

PCI Subjects

PCI subjects were monitored for a 1–2 h period before their PCI procedures, during the procedures, and then during daily-life for 2–4 days thereafter. In two PCI group subjects, the daily-life recordings occurred before their PCI procedures, rather than after. Inflations lasted between 30 and 230 s, with all inflations at the University of Utah lasting approximately 90 s. The treated arteries included: eight left circumflex (LCX), nine right coronary (RCA), and 17 left anterior descending (LAD).

At Borgess, subjects were excluded from the study if balloon inflation did not induce changes in ST-deviation of at least 1 mm in leads V2, V3, I, II or III, which were monitored during the procedure. Six out of 24 Borgess patients were excluded based on these criteria. The inflation times (in seconds) for these disqualified patients were 31, 24, 25, 125, 45, and 180, respectively. The corresponding inflated arteries were: LCX, RCA, RCA, distal LCX, LAD, and LAD. At Borgess, in the case of an ambiguous ST-deviation response during the procedure, long term monitoring was performed, and two out of 18 Borgess patients who were monitored long term were excluded due to a lack of an inflation induced change in ST-deviation of at least 0.1 mV in leads V2, V3, I, II, or III. The arteries were the LCX and posterior descending artery.

For the University of Utah dataset, three of 17 inflations were excluded due to a failure to produce a change in ST-deviation of at least 0.1 mV in leads V2, V3, I, II, or III. The artery in all three cases was the RCA.

Instrumentation

Northeast Monitoring (NEMon) Holter monitors were used for data collection. For the PCI group, Holter monitors were outfitted with radiolucent leads from Vermed, Inc. The sampling rate was 360 Hz, the high pass filter was 0.05 Hz and the low pass filter was 70 Hz. For long term monitoring, 10 s data segments were acquired every 30 s. For short term pre-PCI and PCI monitoring, data was acquired continuously to ensure that the entire inflation sequence was captured.

Data Pre-Processing

In order to emulate the sampling rate limitations of an implantable medical device, the data were down-sampled from 360 to 200 Hz. The data were then processed by an algorithm that automatically detected and removed gaps and very noisy portions in the 10-day Control group recordings. This preprocessing was necessary because the records contained noise due to such factors as electrodes that accidentally fell off or that were temporarily removed to enable subjects to take showers. The pre-processing involved performing beat detection on an entire record and assessing the record's high frequency content by summing the absolute values of the first finite difference of the signal within segments of the data. Segments of data were removed if: (i) the high frequency noise exceeded a first empirically determined threshold, (ii) the number of detected beats within a segment was smaller than physiologically possible, or (iii) the detected beats corresponded to a highly irregular rhythm and the high frequency noise exceeded a second empirically determined threshold. This rejection procedure resulted in the elimination of approximately 5% of the raw data.

For the PCI group, to create a long-term daily-life dataset which could serve as a baseline for detecting inflations, data from the 2-day post-surgical period was inserted into the *beginning* of a patient's record. Long term baseline data was acquired post-procedure rather than pre-procedure mainly due to practical issues pertaining to subject recruitment. The data collected during the PCI interval then followed, with the last 10 s of the inflation repeatedly concatenated into the end of the record in order to form a 10 min interval of data. (In real life, dangerous ischemic events generally last at least 10 min.)

Lead Placement

Figure 1 shows the locations of the two bipolar leads that we used to record data analyzed by our ischemia detection algorithm. The figure shows the leads superimposed on contour maps, published by Horacek *et al.*[6] that represent changes in ST-deviation induced by balloon occlusions of the LAD, RCA, and LCX arteries. In particular, the contour maps show ST-deviation voltages during balloon occlusion minus pre-occlusion ST-deviation voltages. The maps are averages over 15 patients each who experienced LAD, RCA, and LCX balloon occlusions, respectively. Based in part on this data, we selected a "Left Down Lead" (LD) and a "Left Up Lead" (LU). The LD lead records the voltage difference between the anterior left chest (V2 lead position) and the lowest rib along the mid-axillary line while the LU lead records the voltage difference between the anterior left chest and the left superior pectoral region.

Algorithm Overview

The algorithm evaluated here simulated a data collection paradigm suitable for an implanted device. Specifically, in order to conserve both memory and power, 10-s long data segments were processed once every 30 s. The algorithm extracted ST-segment information from each 10-s segment of the daily life data and computed statistically based, heart-rate dependent

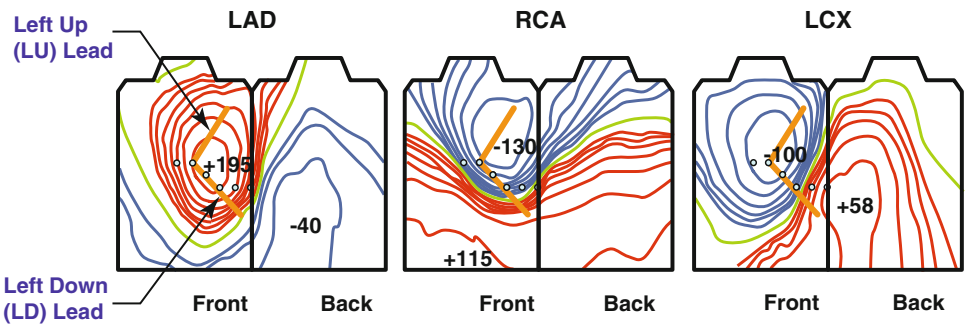

FIGURE 1. Holter electrode placement. The two bipolar leads analyzed for ischemia detection are the "left-down" (LD) and "left-up" (LU) leads, which are shown superimposed on body surface maps of ST-deviation shifts caused by balloon occlusion. The contour maps are averages over groups of 15 patients who experienced LAD, RCA, and LCX balloon occlusions, respectively. Data from Horácek *et al.*[6] Units are μV, contour interval varies.

ischemia detection "metrics" that were functions of the normal variability of ST-deviation. An "acute ischemia" detection occurred when a metric exceeded a corresponding detection threshold for longer than 5 min.

A high level flowchart of the ischemia detection algorithm and associated signal pre-processing is shown in Fig. 2. The initial step involves acquisition of a 10 s data segment, which is then filtered, amplified, and converted to digital form. The first algorithmic step is the assessment of the high frequency noisiness of the segment by summing the absolute values of the first finite difference of the signal for the entire segment, and comparing the result to an empirically determined threshold. Beat detection is performed only on segments that are not too noisy. The RR interval between successive beats is determined, and beats associated with an abnormally short RR interval (e.g., premature ventricular contractions) are excluded from further analysis.

The next step involves examining the QRS morphology of remaining beats by applying tests to various QRS parameters. For example, the time between the maximum positive and maximum negative slopes must be within a selected range for the beat to be analyzed further. The ST-deviation for each accepted sinus beat is then computed according to the voltage difference between automatically determined ST and PQ portions of each beat (described below). The ST-deviation of an exemplary beat is shown in Fig. 3.

The ST-deviation of each beat is then compared to both the last value in the filtered ST-deviation time series (labeled "Current Long Term ST Deviation" in Fig. 2) and the median long term ST-deviation (computed over a multi-hour prior time period), to ensure that the beat's calculated ST-deviation is close to at least one of these ST-deviation measures. (This test is not performed during an initialization phase because no long term long-term ST-deviation is yet available.) If the current beat's ST-deviation varies substantially from both of these measures, its ST-deviation value is likely the result of noise and is thus rejected. The ST-deviations of accepted beats are averaged to generate an ST-deviation value for the current segment, which is provided to an exponential average filter, which updates the ST-deviation time series ("Current Long Term ST Deviation").

For each of a number of non-overlapping heart rate ranges, the system maintains ST-deviation statistics. This scheme allows heart rate dependence of ST-deviation to be taken into account. To determine the heart rate range associated with a current segment, the average segment heart rate is computed and then provided as an input to an exponential average filter. The output of the exponential average filter is the current long term heart rate (labeled as such in Fig. 2) which determines the heart rate interval associated with the current long term ST-deviation.

Once a day, the ST-deviation statistics are analyzed to determine a person's normal ranges of heart-rate

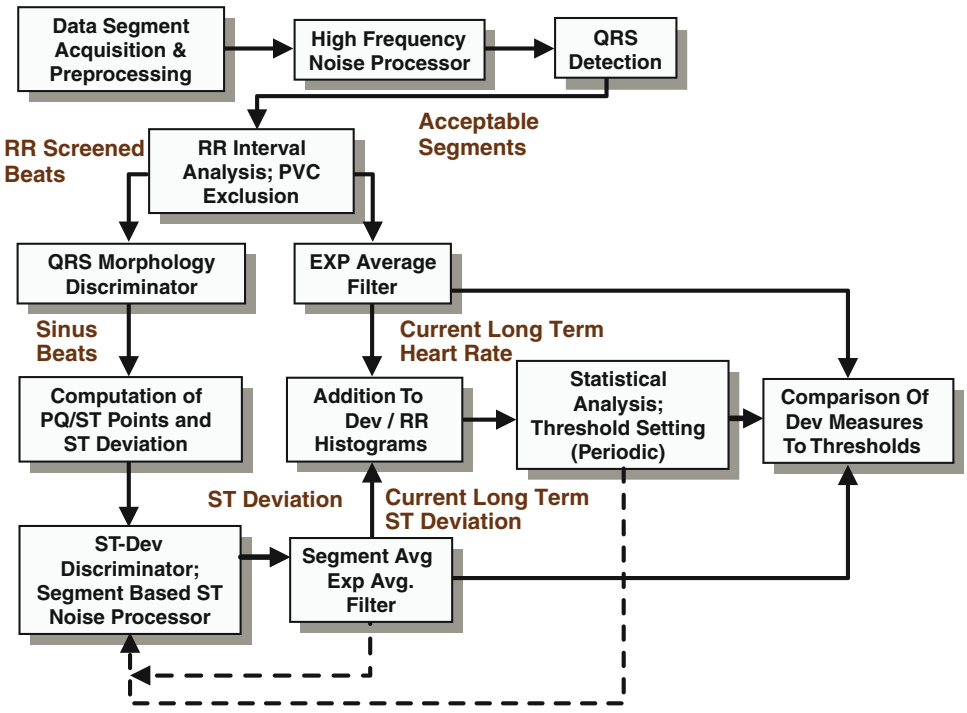

FIGURE 2. Algorithm flowchart. A block diagram of the acute ischemia detection algorithm. Dashed lines indicate feedback. See text for details.

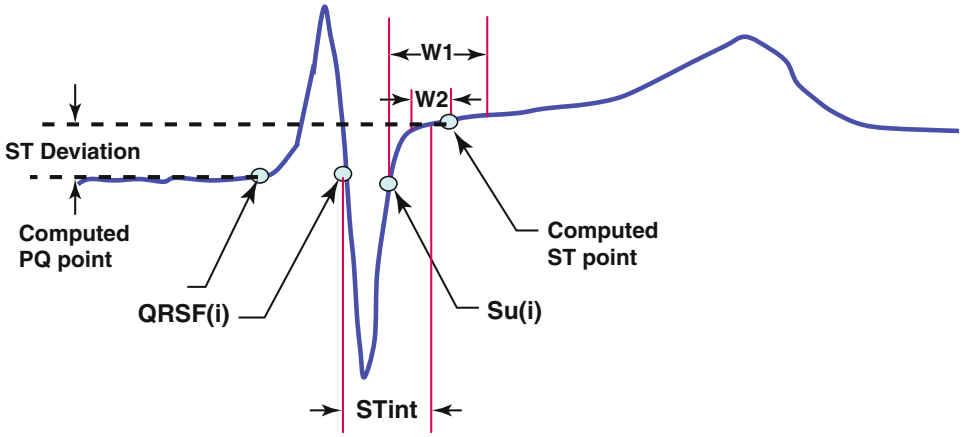

FIGURE 3. Beat fiducial points. A heart beat ECG tracing marked with various points and windows associated with the computation of the ST point. See text for details.

dependent ST-deviation. In the final step, ischemia detection metrics are computed based on both the current long term ST-deviation and the normal range of ST-deviation for that heart rate. More specifically, the ischemia detection metrics are functions of the "distance" between the current long term ST-deviation and the upper and lower boundaries of ST-deviation for a particular subject. Separate metrics are formed for the LD and LU leads, respectively. Metrics that combine information from the two leads are also generated. Both the separate lead metrics and combination lead metrics are compared to respective thresholds, and the algorithm detects acute ischemia when any one of the metrics is above its threshold for at least 10 consecutive segments, which is equivalent to 5 min (30 s/segment × 10 segments = 300 s).

As will be further described below, the algorithm requires various parameter values to generate ST-deviation vs. heart rate histograms. All of these parameter values were set based on a combination of theoretical and empirical considerations. The same parameter values were applied to both Control and PCI data sets.

PQ/ST Segment Determination

With regard to the Fig. 2 flowchart, the determination and measurement of PQ and ST points are performed in the block labeled "Computation of PQ/ST Points and ST Deviation." Both PQ and ST points are automatically determined by locating waveform regions of low curvature within a fixed window referenced to a QRS fiducial point. These candidate regions are then adjusted based on the ST and PQ point locations of previously processed QRS complexes. The adjustment ensures that the locations of ST and PQ points, relative to a QRS fiducial point, are similar from beat to beat.

For a discrete signal $x(n)$, the ST point for the ith QRS complex in the jth data segment is searched within a fixed window ($W1$) defined $W1 = [Su(i) + a, Su(i) + b]$, where Su is a point on toward the end of the QRS complex and a and b are positive integers subject to $b > a$. Exemplary values of a and b are 2 and 12 samples, respectively. $W1$ and Su are shown in Fig. 3, which is a sample QRST waveform. The typical QRS shape for both of the candidate leads (LD and LU in Fig. 1) is characterized by a large final upstroke known as an S wave. For these QRS complexes, Su is the first sample after the nadir of the S wave at which $x'(k1) < c^*x'(Smax(i))$, where $Smax(i)$ is the sample at which the first finite difference of the ith QRS S wave reaches its maximum value, $x'(k1)$ is the first finite difference of signal $x(n)$ at sample $k1$, and c is an empirically determined parameter that we set at 5/8.

Within $W1$, a search is performed for consecutive samples at which the second finite difference of the waveform is less than a threshold that is referenced to QRS amplitude: $|x''(n)| < d^*QRSAav(j)$, where $QRSAav(j)$ is the average QRS amplitude of normal beats within the jth segment and d is an empirically determined parameter that we set to 1. If consecutive samples ($k2$, $k3$) satisfying this condition are found, then the ST point (ST) is set according to $k1$ and an adaptive window ($W2$). In particular, if $k2$ falls within $W2$, then $ST(i)$ is set equal to $k2$. If $k2$ is outside of $W2$, then $ST(i)$ is set equal to whichever of the boundaries of $W2$ is closer to $k2$. The equation for the ST point (when a qualifying pair of samples ($k2$, $k3$) is found), is as follows:

$$ST(i) = \max(\min(k2, \max(W2)), \min(W2)), \quad (1)$$

where $W2 = [QRSf(i) + STint(t)\text{-}c, \quad QRSf(i) + STint(t) + d]$, $QRSf(i)$ is the index of a QRS fiducial point for beat i, c and d are positive integers that we set to the value of 1, and $STint(t)$ is the current value (at discrete time index t) of an average of past values of the QRS to ST interval: $ST() - QRSf()$. $STint$ is then updated according to an exponential average filter:

$$STint(t+1) = \alpha * STint(t) + (1-\alpha) * (ST(i) - QRSf(i)) \quad (2)$$

STint is initialized to an empirically determined value. For dominant S wave QRS morphologies, $QRSf(i)$ is equal to the index at which the slope of the QRS of beat i reaches its minimum value.

PQ points are determined in an analogous manner. ST-deviation is then set equal to the difference in average signal amplitude at the three samples centered on the ST and PQ points respectively. Figure 3 diagrammatically shows ST-deviation with respect to a particular heart beat.

Ischemia Detection Metrics—"Distance Markers"

The general detection strategy was to compare the ST-deviation of current heart beats with previously determined normal upper and lower boundaries for a person's ST-deviation. With regard to Fig. 2 flowchart, this analysis occurs in the block labeled "Statistical Analysis; Threshold Setting (Periodic)." Ischemia detection metrics were based on the "distance" between a current ST-deviation measurement and these (heart rate dependent) boundaries that define a normal state of each patient. We tested two types of "distances": an absolute distance from the boundary (e.g., if a current ST-deviation is 0.1 mV beyond a boundary, the metric's value is 0.1 mV); and a relative distance from the boundary, based on the dispersion of the data (e.g., if a measure of the dispersion is 10 U, and a current ST-deviation is 2 U beyond a boundary, then the relative metric is 2/10 = 0.2).

Relative distances were determined by "distance markers." Returning to the above example, the 10 U measure of dispersion is a "distance marker." Details of the relative distance marker calculation process will be described with reference to Fig. 4, which is a plot of ST-deviation vs. heart rate derived from 2 days of LD lead data from a Control subject. The y-axis value for each point (blue circle) in the plot is a "Current long term ST-deviation" value (Fig. 2) while the x-axis value is the corresponding "Current long term heart rate" value.

The algorithm for computing relative distance markers divides the heart rate into between 10 and 12 non-overlapping bins $B1$, $B2$,…,BN. For example, in

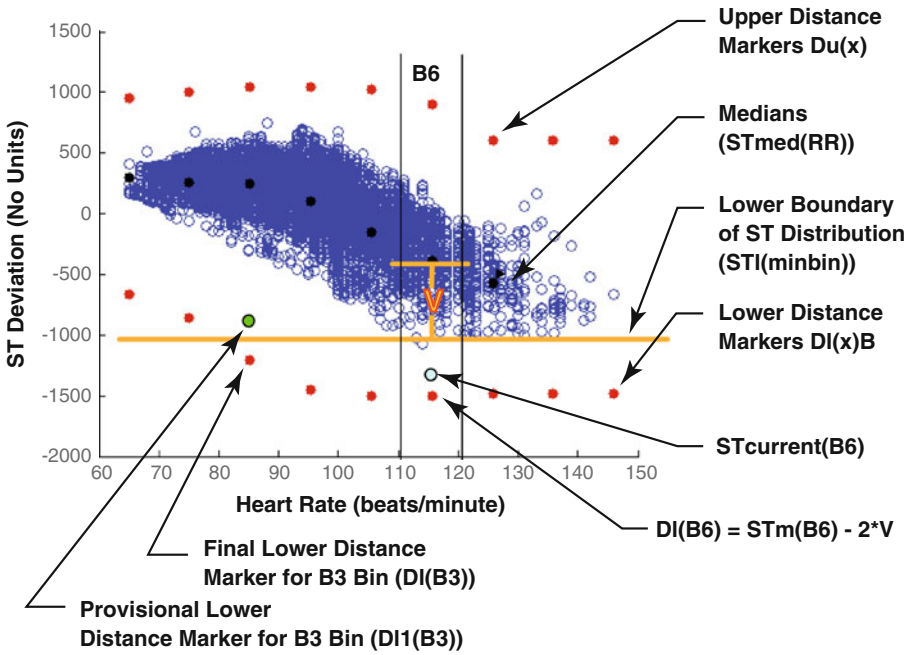

FIGURE 4. A scatter plot of filtered ST-deviation vs. filtered heart rate for a subject from the Control group. The upper and lower series of red circles are "distance markers" that form the basis for computing relative ischemia detection "metrics." An ischemia detection metric is a measure of the abnormality of a particular ST-deviation measurement. Higher values of the metric correspond to greater levels of abnormality. If a current ST-deviation measurement is within the normal range (e.g., within the cluster of blue circles) for a given heart rate, the metric value is 0. If a current ST-deviation measurement is outside of the normal range but not beyond the pertinent red circle, the metric value is between 0 and 1. If a current ST-deviation measurement is beyond the pertinent red circle, the metric value is greater than 1.

Fig. 4, the sixth bin ($B6$) includes values associated with the heart rate range from about 111 to 121 beats per minute. The median ST-deviation for each bin x ($STm(Bx)$) is computed. The upper and lower boundaries for each bin are then computed by determining the ST-deviation values above and below which there are only a small number (e.g., 10) of points. This boundary location approach was implemented because the ST-deviation data is non-Gaussian (due in part to exponential averaging of the ST-deviation time series) and tends to be characterized by relatively sharp boundaries with outlier points that result from noise.

For each bin x with at least a minimum number (Na) of elements, provisional upper and lower "distance markers", denoted by $Du1(Bx)$ and $Dl1(Bx)$ respectively, are set based on measures of the dispersion of the data that are functions of the bin medians (STm) and the upper and lower boundaries STu and STl, respectively. In particular, $Du1(Bx) = STm(Bx) + 2*(STu(Bx) - STm(Bx))$ and $Dl1(Bx) = STm(Bx) + 2*(STl(Bx) - STm(Bx))$. In Fig. 4, $(STl(B6) - STm(B6))$ is indicated by the label V.

The provisional distance markers are then adjusted in two ways. First, both positive and negative distance markers for a particular heart rate bin (e.g., B6) are adjusted based on the upper and lower boundaries of ST-deviation over all heart rate bins. The use of this global upper and lower boundary information enables all distance markers to be set based on a relatively larger data set, i.e., the set of all ST-deviations over all heart rate bins, than the data in a single heart rate bin. The final upper and lower distance markers (for bins with at least Na elements) for bin x is:

$$Dl(Bx) = Dl1(Bx) - (Dl1(Bx) - Dl1(maxbin)) * \min(1, (Dl1(Bx) - Dl1(maxbin))/S) \quad (3)$$

$$Du(Bx) = Du1(Bx) + (Du1(maxbin) - Du1(Bx)) * \min(1, (Du1(maxbin) - Du1(Bx))/S) \quad (4)$$

where $Du1(maxbin)$ and $Dl1(maxbin)$ are the provisional distances for the bin with the largest lower and upper ST-deviation boundaries, respectively and S is a parameter that governs the amount of adjustment. The value of the parameter S depends on the range of ST-deviation; if that range is 1000, then a preferred value for S is 2000. Na is an empirically determined parameter that was set at 10. According to the above equation, the closer that a provisional distance is to the maximum distance marker, the less the adjustment. Figure 4 shows an example of the global adjustment effected by Eqs. (3) and (4). The provisional distance marker for bin B3 is labeled.

Second, lower distance markers $Dl1(Bx)$ are adjusted to enhance sensitivity to ST depression if subjects did not exhibit ST depression during the baseline period in a particular lead. In particular, for these subjects/leads, the lower distance markers were increased according to:

$$Dl(x) = \max(Dl(x), STl(minbin) - W), \quad (5)$$

where W is a parameter that depends on the range of ST-deviation; if that range is 1000, then a preferred value for W is 200. The application of Eq. 5 may result in the increase of lower distance markers, which in turn makes it more likely that even slight negative ST-deviations will be detected as acute ischemia. If there are less than Na points in a particular bin corresponding to a particular heart rate range, then ischemia detection did not occur when the heart rate was within the range.

Final Ischemia Detection Metrics

Relative metrics are based on the distance markers (Eqs. (3)–(5)) and result in a unitless measure of the degree of abnormality of a current ST-deviation. For example, a positive ST-deviation in the LD lead may be 75% beyond a person's normal (heart rate dependent) LD lead upper ST-deviation boundary, measured as a percentage distance to the upper distance marker.

More specifically, the final upper and lower metrics ($Mu(Bx)$ and $Ml(Bx)$) that are compared to thresholds to detect ischemia are:

$$Ml(Bx) = \max(0, (STcurrent(Bx) - STl(Bx))/(Dl(Bx) - STl(Bx))) \quad (6)$$

$$Mu(Bx) = \max(0, (STcurrent(Bx) - STu(Bx))/(Du(Bx) - STu(Bx))) \quad (7)$$

Thus, for example, if a current ST-deviation is below the upper boundary ($STu(Bx)$), then $Mu(Bx)$ is 0. As an example of an ST-deviation that results in a positive metric, in Fig. 4, the $Ml(B6)$ for the data point labeled as "E" is approximately 0.75. To detect acute ischemia, this value of 0.75 is then compared to a threshold.

The ST-deviation metrics of individual leads were combined by simple addition to derive combination metrics. There are four possibilities: (1) both leads are characterized by relative ST elevation, in which case $Mu(Bx)_{,\mathrm{LD}} > 0$ and $Mu(Bx)_{,\mathrm{LU}} > 0$, where the amended subscript refers to the relevant lead (LD or LU); (2) the LD and LU leads are characterized by relative ST elevation and ST depression, respectively, in which case $Mu(Bx)_{,\mathrm{LD}} > 0$ and $Ml(Bx)_{,\mathrm{LU}} > 0$; (3) the LD

and LU leads are characterized by relative ST depression and ST elevation, respectively, in which case $Ml(Bx)_{,LD} > 0$ and $Mu(Bx)_{,LU} > 0$; and (4) both LD and LU leads are characterized by relative ST depression, in which case $Ml(Bx)_{,LD} > 0$ and $Ml(Bx)_{,LU} > 0$. Therefore, the corresponding four "combination metrics" are: (1) $Mu(Bx)_{,LD} + Mu(Bx)_{,LU}$; (2) $Mu(Bx)_{,LD} + Ml(Bx)_{,LU}$; (3) $Ml(Bx)_{,LD} + Mu(Bx)_{,LU}$; and (4) $Ml(Bx)_{,LD} + Ml(Bx)_{,LU}$.

The absolute detection metrics for individual leads are:

$$MAl(Bx) = \max(0, (STl(B) - STcurrent(Bx))) \quad (8)$$

$$MAu(Bx) = \max(0, (STcurrent(Bx) - STu(Bx))) \quad (9)$$

The 12 ischemia detection metrics are listed in Table 1.

Metric Evaluation

The baseline period for establishing distance markers was 2 days for both the Control group and the PCI group. For each Control group subject, the maximum value of each of the 12 metrics was computed during the entire post-baseline period (e.g., all recorded data not included in the 2-day window used to create the distance markers). For each PCI group subject, the maximum value of each of the 12 metrics was computed over the balloon inflation period. In order to determine the maximum value of a metric for a particular artery, the maximum value of the metric was computed for each heart rate bin, and the maximum value of the metric for that artery was the maximum of this set. Within a particular heart rate bin, the maximum values of the *Mu* and *MAu* metrics were calculated according to the pertinent metric equation (Eqs. (7) or (9)) with the *STcurrent* variable set equal to the ST-deviation of the 10th most positive ST-deviation value within the heart rate bin. The maximum values of the *Ml* and *MAl* metrics were calculated in an analogous manner.

Ten segments of data correspond to 5 min, which is the minimum duration required in our study to detect ischemia. Accordingly, at least ten consecutive segments must exceed threshold before ischemia is detected. Thus, the ST-deviation of the tenth most positive segment is a reasonable choice for assessing the detection capability of the algorithm. (Similarly, as previously described in the Methods section, the 10th most positive ST-deviation defined the upper ST-deviation boundary for each heart rate bin.) Analogously, the *Ml* and *MAl* metrics were calculated with the tenth lowest ST-deviation value within the heart rate bin.

TABLE 1. The 12 detection metrics.

Metric	Description	Threshold (at 0.5 safety factor)
$Mu_{,LD}$	LD lead relative metric for upper boundary	1.4
$Ml_{,LD}$	LD lead relative metric for lower boundary	1.0
$Mu_{,LU}$	LU lead relative metric for upper boundary	2.2
$Ml_{,LU}$	LU lead relative metric for lower boundary	2.7
$Mu_{,LD} + Mu_{,LU}$	Both leads' ST deviation above respective upper boundaries	2.6
$Mu_{,LD} + Ml_{,LU}$	LD lead ST deviation above LD lead upper boundary; LU lead ST deviation below LU lead lower boundary	0
$Mu_{,LU} + Ml_{,LD}$	LD lead ST deviation below LD lead lower boundary; LU lead ST deviation above LU lead upper boundary	0.96
$Ml_{,LU} + Ml_{,LD}$	Both leads' ST deviation below respective lower boundaries	1.16
$MAu_{,LD}$	LD lead absolute metric for upper boundary	51 μV
$MAl_{,LD}$	LD lead absolute metric for lower boundary	63 μV
$MAu_{,LU}$	LU lead absolute metric for upper boundary	201 μV
$MAl_{,LU}$	LU lead absolute metric for lower boundary	338 μV

Performance Measures

Our assessment of algorithm performance was premised on the constraint that false positive ischemia detections were unacceptable. A false positive would have occurred if ischemia had been detected (using thresholds computed with the first 2 days of daily-life data) in any Control group subject in any of the last 8 days of data.

To avoid false positives for each of the detection metrics, the maximum value of each detection metric (*Mmax*) was computed over all Control subjects over the last 8 days of control subject data. We then created a performance measure based on the percentage of proper detections (i.e., number of detections/number of responding inflations) as a function of the "distance" from *Mmax*: percentage of true positive detections with a detection threshold set at $(1 + SF)^* Mmax$, where *SF* is a "safety factor" parameter that varied from 0 to 5. Setting SF to 0 would cause the performance measure to be assessed using a threshold set at the maximum value for a detection metric across

our 14 Control subjects, such that a false positive in the Control group is avoided without any safety margin.

RESULTS

Ischemia Detection

Table 2 summarizes the responding arteries and detections with the safety factor set to 0.5. The algorithm detected 17/17 LAD occlusions, 7/8 LCX occlusions, and 8/9 RCA occlusions. Note that four patients each had two different arteries obstructed by balloon inflation, so the 34 arteries correspond to 30 different patients.

Figure 5a shows the ranges of ST-deviation (over all heart rates) in the LD lead. The range of ST-deviation which occurred during the baseline is coded in blue. The minimum (green) and maximum (red) values seen in the post-baseline periods are also shown for both Control subjects and patients (classified by occluded artery). In 4 patients, there were inflations in two different arteries rather than in a single coronary artery. Accordingly, the baseline range (blue) is the same for both arteries of the pair (e.g., the 2nd and 3rd from the top in the LAD group correspond to the same individual; the inflation of this patient's diagonal branch of the LAD was considered separately from the inflation to the middle portion of the main LAD). In the Control subjects, the maximum and minimum ST-deviation values recorded during both the baseline and post-baseline periods (i.e., across the full 10 day period) were approximately 190 and -20 μV, respectively for the LD lead. In the Control group, during the baseline period, the ST-deviation for any individual subject did not exceed a total range of 100 μV, and the average total range across subjects was 79 μV. Within the Control group, the greatest difference between post-baseline maximum and baseline maximum (i.e., largest red bar) was 23 μV while the greatest difference between post-baseline minimum and baseline minimum was 20 μV (i.e., largest green bar).

TABLE 2. True positive detections with the Safety Factor set to 0.5.

Artery	Detections (SF = 0.5)	Transmural ischemia (ST-elevation over affected artery)/ subendocardial ischemia
LAD (main branch)	15/15	14/1
LAD (first diagonal)	2/2	2/0
LCX (posterior)	5/6	5/0
LCX/Ramus (lateral)	2/2	2/0
RCA	8/9	9/0
Total	32/34 (=0.94)	33/1

During baseline recordings, the PCI patients generally showed a wider range of ST-deviations than the Control group. LAD inflations produced ST-deviations of >200 μV in 11/17 subjects. RCA or LCX inflations produced ST depression in 15/17 subjects whereas 14/17 of the RCA and LCX records exhibited no ST depression during the baseline period.

Figure 5b shows analogous data for the LU lead. Compared to the LD lead, the LU lead data generally shows a smaller dispersion in baseline ST-deviation with an average range across Control subjects of 63 μV. However, for the PCI group, the greatest difference between the baseline and post-baseline maximum (red boxes) was 33 μV, with the greatest difference between the baseline and post-baseline minimum (green boxes) differing by 32 μV. Both of these ST-deviation related differences between baseline

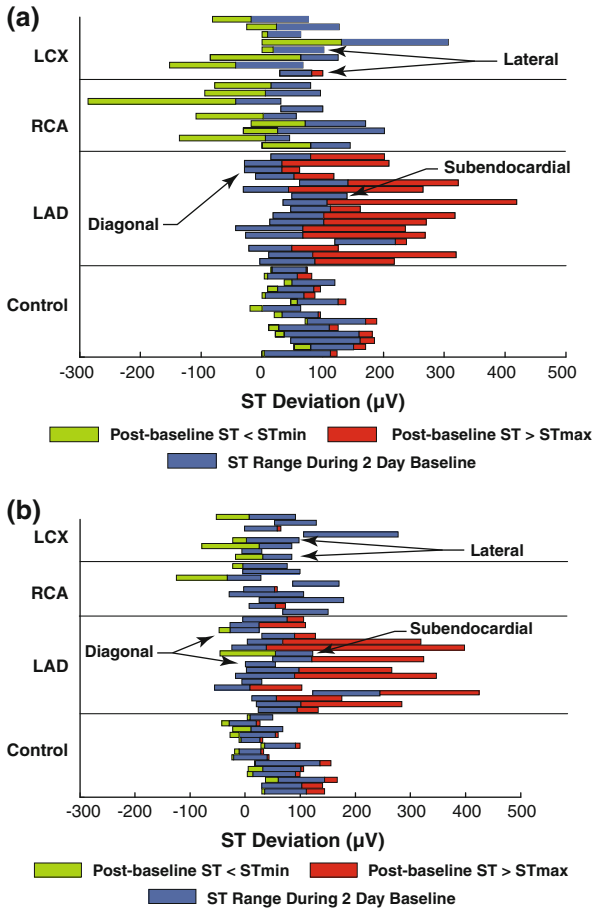

FIGURE 5. (a, b) Maximum and minimum changes between baseline to post-baseline conditions. Bar chart of baseline (blue) and post-baseline/inflation maximum (red) and minimum (green) ST-deviation values for the LD and LU leads respectively for each subject/artery. The maximum and minimum ST-deviations over all heart rate ranges during the baseline period are denoted by STmax and STmin, respectively. If the post-baseline/inflation maximum or minimum ST-deviation is less than STmax or greater than STmin, respectively, then there is no red or green bar.

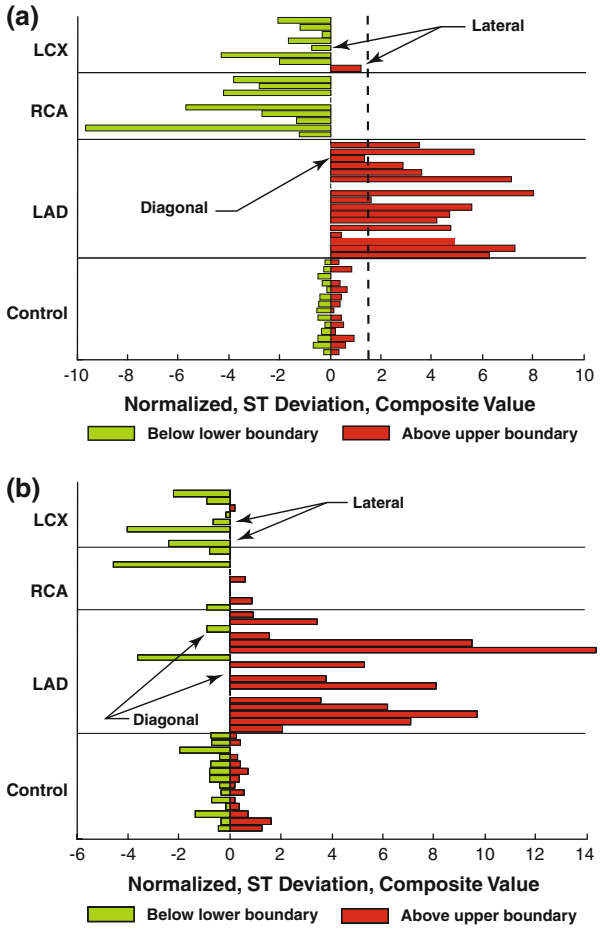

FIGURE 6. (a, b) Relative metrics. Bar chart of maximum (red) and minimum (green) relative metric values over the entire post-baseline/inflation period for the LD and LU leads respectively for each subject/artery. See text for further details.

and PCI conditions are about 50% larger than those found for the LD lead.

LAD inflations produced ST elevation in the LU lead in most (13 of 17) subjects. In subject 18, an LAD inflation produced substantial ST elevation in the LU lead but only a small ST change in the LD lead. One inflation of the mid-LAD ("Subendocardial" in Fig. 5b) produced ST depression in the LU lead without any substantial change in the LD lead.

Overall, the LU lead was less sensitive to RCA and LCX occlusions than the LD lead. However, in two lateral occlusions within the LCX group (one obtuse marginal and one Ramus branch) the LU lead was more sensitive than the LD lead. In particular, for these two occlusions, the LU lead registered ST depression whereas the LD lead registered moderate ST elevation (see lower of the two "Lateral" arrows in Figs. 5a and 5b) and slight ST depression (see upper of the two "Lateral" arrows in Figs. 5a and 5b).

Figure 6a shows the maximum and minimum post-baseline values of the LD relative detection metrics.

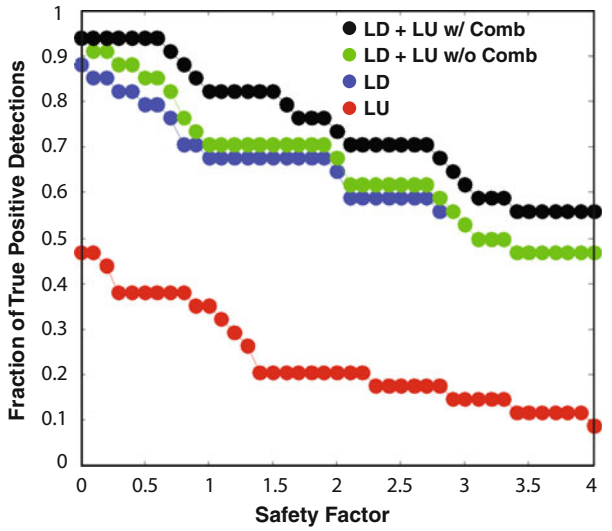

FIGURE 7. Performance curves. Percentage of proper detections without false positives for different combinations of leads and metrics. The "safety factor" is a measure of "distance" between the detection threshold (to which metrics are compared) and the smallest threshold that will avoid false positives. A "safety factor" of 0 means that the detection threshold is just slightly above the level that avoids any false positive detections in the control group.

For the PCI group, the figure shows only the largest values of the metric that were found within the data collected during PCI inflations. The dashed vertical line in Fig. 6a represents an ischemia detection threshold of 1.4 for $Mu_{,\mathrm{LD}}$, which corresponds to a safety factor of 0.5 (See Table 2). At this threshold, use of the $Mu_{,\mathrm{LD}}$ metric would detect 14/17 LAD occlusions without causing a false positive in the control group. Figure 6b shows corresponding results for the LU lead.

Figure 7 plots the true positive detections of ischemia which occurred in the PCI data as a function of the safety factor for the LD and LU leads separately (blue and red, respectively). Detections which rely upon a rule which requires either lead to detect ischemia for a true detection to occur (i.e., the union of detections) is plotted in green. Using both the union of the detections and also utilizing the combination metrics described in Table 1 led to detection results shown in black. For the separate leads, both relative (metrics 5–8) and absolute (metrics 9–12) ischemia detection metrics listed in Table 1 were used. In each subject, if at least one absolute or relative metric was above threshold then the result was a successful detection.

Non-Responders

Three of the 11 patients whose data were excluded from the analysis had LCX occlusions. The remaining 8 had LAD or RCA (with one a posterior descending ar-

tery) occlusions. For five of the non-responders who were monitored long term, both the LD and LU leads, as well as limb leads I, II and III, and precordial lead V2, were examined for evidence of any inflation induced ST shift. In all of these patients except for one, none of the leads showed an inflation induced ST shift of even 0.05 mV. One patient, who had an RCA inflation, exhibited at least 0.1 mV of negative ST shift in lead V2 relative to the ST-deviation level at inflation onset. This patient showed a large increase in ST-deviation that started shortly before inflation onset; the maximum inflation induced ST-deviation was not substantially different than the pre-catheterization ST-deviation.

DISCUSSION AND LIMITATIONS

Our results suggest that automatically generated, patient specific, heart-rate dependent ST-deviation thresholds can detect myocardial ischemia that results from balloon inflations, without false positive detections in a small Control group. Our data does not establish that the detection of ischemia would occur with a similar efficacy in the detection of ambulatory acute ischemic events. First, our Control group consisted of 14 people, a relatively small population. A larger control group might have resulted in larger *Mmax* values, which in turn would have shifted the performance curves in Fig. 7 lower. Second, balloon inflation recordings were made on supine, motionless subjects in a relatively noise free environment; real life recordings might be noisier. Also, our daily-life (baseline) recordings for the PCI group were made during a two day post-operation period, during which many subjects may have been relatively sedentary due to their recent surgeries. This may have resulted in relatively decreased dispersions of ST-deviation data, which would have improved our results compared to real life situations. On the other hand, the short duration of the balloon inflations may have resulted in ST-deviations smaller than those of real-life ischemic events.

The statistically based ischemia detection approach mitigates the effects of "noise" sources such as axis shifts and slow ST-deviation drift. The ST-deviation values that result from these sources tend to become part of an individual's baseline ST-deviation statistics and therefore do not result in false positive ischemia detections. Of course, if axis shifts result in very large dispersions of ST-deviation, then ischemia detection thresholds will be higher, and detection sensitivity correspondingly reduced. Axis shifts within our dataset resulted in ST-deviation dispersions that were far smaller than the changes induced by PCI.

ST-deviation changes resulting from many types of conduction abnormalities that affect QRS duration are mitigated by performing QRS morphology checks and excluding abnormal beats from ischemia detection. To the extent that a conduction abnormality doesn't substantially affect QRS duration but causes an ST-deviation change, the corresponding ST-deviation values may become part of an individual's baseline statistics. The resulting effect on the algorithm is similar to that of axis shifts: a larger ST-deviation dispersion will reduce detection sensitivity.

It is known that some patients may not develop significant ST shifts during balloon inflations (termed "non-responders"). We cannot rule out ischemia in the non-responder group, especially for the LCX occlusions. If all three excluded LCX patients are considered false negatives, then each of the detection percentages shown in Fig. 7 should be reduced by 0.08 (3/37).

In conclusion, we have shown that an algorithm based on patient specific, heart-rate dependent ST-deviation thresholds can accurately detect balloon inflations in a relatively small dataset. Future work will involve testing the algorithm on larger datasets.

ACKNOWLEDGMENTS

This work was funded in part by SBIR grant 1R43HL096158-01 from the National Heart, Lung and Blood Institute of the National Institutes of Health. The contents of this work are solely the responsibility of the authors, and do not necessarily reflect the official views of the NIH or the NHLBI. The authors would like to thank Renee Neuharth, RN and Sandy Wilson, RN, the study coordinators at the University of Utah and Borgess Medical Center respectively. The authors would also like to thank Milan Horácek for providing the body-surface datasets that were used to help select the bipolar leads assessed in this study. Finally, the authors would like to thank Rob Granger at Angel Medical Systems for his help in preparing the figures in this paper.

CONFLICT OF INTEREST

BH, MSJ, and SRJ have received SBIR phase I and II grants related to this work. BH, MSJ, TAF, and SRJ are employees of, and own stock in, Angel Medical Systems (AMS). AMS is developing a subcutaneous ischemia monitor.

REFERENCES

[1]ACC/AHA. Guidelines for the management of patients with unstable angina and non-ST-segment elevation myocardial infarction. *J. Am. Coll. Cardiol.* 36:970–1062, 2000.

[2]American Heart Association. Guidelines for cardiopulmonary resuscitation and emergency cardiovascular care. Part 8: Stabilization of the patient with acute coronary syndromes. *Circulation* 112:IV-89–IV-110, 2005.

[3]Fischell, T. A., D. R. Fischell, A. Avezum, M. S. John, D. Holmes, M. Foster, III, R. Kovach, P. Medeiros, L. Piegas, H. Guimaraes, and C. M. Gibson. Initial clinical results using intracardiac electrogram monitoring to detect and alert patients during coronary plaque rupture and ischemia. *J. Am. Coll. Cardiol.* 56(14):1089–1098, 2010.

[4]Fischell, T. A., D. R. Fischell, R. E. Fischell, R. Virmani, J. J. DeVries, and M. W. Krucoff. Real-time detection and alerting for acute ST-segment elevation myocardial ischemia using an implantable, high-fidelity, intracardiac electrogram monitoring system with long-range telemetry in an ambulatory porcine model. *J. Am. Coll. Cardiol.* 48(11):2306–2314, 2006.

[5]Hopenfeld, B., M. S. John, D. R. Fischell, P. Medeiros, H. P. Guimarães, and L. S. Piegas. The Guardian: an implantable system for chronic ambulatory monitoring of acute myocardial infarction. *J. Electrocardiol.* 42(6):481–486, 2009.

[6]Horácek, B. M., J. W. Warren, C. J. Penney, R. S. MacLeod, L. M. Title, M. J. Gardner, and C. L. Feldman. Optimal electrocardiographic leads for detecting acute myocardial ischemia. *J. Electrocardiol.* 34(Suppl):97–111, 2001.

[7]Laguna, P., G. B. Moody, R. Jané, P. Caminal, and R. G. Mark. Karhunen-Loève transform as a tool to analyze the ST-segment. Comparison with QT interval. *J. Electrocardiol.* 28(Suppl):41–49, 1995.

[8]Maglaveras, N., T. Stamkopoulos, K. Diamantaras, C. Pappas, and M. Strintzis. ECG pattern recognition and classification using non-linear transformations and neural networks: a review. *Int. J. Med. Inf.* 52(1–3):191–208, 1998.

[9]Smrdel, A., and F. Jager. Automatic classification of long-term ambulatory ECG records according to type of ischemic heart disease. *Biomed. Eng. Online* 10(1):107, 2011.

[10]Song, Z., J. Jenkins, M. Burke, and R. Arzbaecher. The feasibility of ST-segment monitoring with a subcutaneous device. *J. Electrocardiol.* 37(Suppl):174–179, 2004.

[11]Stadler, R. W., S. N. Lu, S. D. Nelson, and L. Stylos. A real-time ST-segment monitoring algorithm for implantable devices. *J. Electrocardiol.* 34(Suppl):119–126, 2001.